Mechanics of Advanced Composite Structures

The Effect of Temperature Dependency on the Thermo-Electro-Elastic Analysis of Functionally Graded Piezoelectric Spherical Shell

M. Arefi [*], **M. Takhayor Ardestani**

Department of Solid Mechanic, Faculty of Mechanical Engineering, University of Kashan, Kashan 87317-51167, Iran

PAPER INFO

ABSTRACT

Results of electro-thermo-elastic analysis of a functionally graded thick-walled spherical shell made of temperature dependent materials are presented in this article. All material properties are assumed temperature-dependent and also are graded along the thickness direction based on power function. Temperature dependency is accounted for all material properties including, thermal, mechanical and electrical properties based on linear variation. Thermal conduction relation is solved using thermal boundary conditions at inner and outer radii for temperature dependent and independent cases. Substitution of temperature distribution into constitutive relations and then into equilibrium and Maxwell equations would give final governing equations having variable thickness. The variable coefficient governing equations are solved using the division method. The numerical results are presented for both temperature-dependent and temperature-independent cases so as to investigate the effect of temperature dependencies. The results indicate that considering temperature dependency would lead to significant changes in responses including radial and circumferential displacements and stresses, electric potential and temperature distribution.

1. Introduction

Functionally graded materials have been produced for simultaneously bearing thermal and mechanical loads in a structure with high gradient of temperature. The experiments indicate that temperature variation can significantly change the various characteristics (mechanical, thermal and electrical properties) of materials rather than room temperature. This change would lead to significant change of materials behavior and responses of structures made of them subjected to various loadings. A literature review on the previous works related to thermo-electro-elastic analysis of piezoelectric structures indicates that researchers have not comprehensively and analytically investigated the

temperature dependency. In this section, a literature review on temperature dependent works and on the thermo-electro-elastic analysis of various structures are presented in order to show the importance of this work.

Teyssedre and Lacabanne [1] studied the behavior of thermal and dielectric P(VDF-TrFE) copolymers in relation with their electroactive properties. Tanigawa et al. [2] presented the transient heat conduction and thermal stress analysis of inhomogeneous materials with temperature dependent material properties. They showed that accounting the thermal conductivity would lead to a nonlinear differential equation. Substitution of temperature distribution using solution of nonlinear differential equation into stress components and then

---
[*] Corresponding author. Tel.: +98-31-55913405; Fax: +98-31-55913400
E-mail address: arefi63@gmail.com, arefi@kashanu.ac.ir

into equations of motion leads to transient thermal stress distribution.

Omote et al. [3] presented the properties of the elastic, dielectric, and piezoelectric of poly (vinylidine fluoride-trifluoroacetylene) shells in the form of graphs with temperature dependency. Wong et al. [4] examined Specific heat and thermal diffusivity of Vinylidene Fluoride/Trifluoroethylene Copolymers. Thermal post-buckling analysis of functionally graded cylindrical thin shell with considering temperature dependency and finite length subjected to uniform temperature distribution was studied by Shen [5]. Nonlinearity was accounted in derivation of governing equations of motion using von Kármán–Donnell-type of kinematic nonlinearity. Buckling temperature and postbuckling load–deflection curves were determined based on a singular perturbation technique.

Liew et al. [6] studied thermal postbuckling analysis of laminated plate made of functionally graded materials. Temperature dependency was accounted for material properties. Kim [7] studied vibration characteristics of functionally graded rectangular plate with initial stress. The plate was assumed to be made of metal and ceramic considering temperature dependency. The material properties were assumed to be graded along the thickness direction based on power law distribution. The Rayleigh–Ritz procedure was applied to obtain the frequency equation. The double Fourier series was employed to examine the effect of material compositions, plate geometry, and temperature fields on the vibration characteristics of functionally graded rectangular plate. Thermo-mechanical post-buckling analysis of cylindrical panels made of functionally graded materials considering temperature dependency was studied by Yang et al. [8] based on classical shell theory with von-Karman–Donnell-type nonlinearity. Differential quadrature method was utilized for solution of the problem. The parametric numerical results were presented to study the effects of temperature-dependent properties, volume fraction index, axial load, initial imperfection, panel geometry and boundary conditions on the thermomechanical post-buckling behavior.

Shen [9] studied thermal post-buckling analysis of a functionally graded plate with simply supported boundary condition based on higher-order shear deformation theory subjected to two types of temperature distribution. Temperature dependency and power law function were used for material properties. The buckling and post-buckling temperatures were calculated based on a two-step perturbation technique. It was concluded that considering the temperature dependency would lead to significant

improvement of results rather than the case in which the temperature dependency is ignored.

Dynamic buckling analysis of functionally graded temperature dependent cylindrical shell with geometric imperfection and integrated with sensor and actuator layers was studied by Shariyat [10]. The numerical results were presented to investigate the influence of temperature dependency, volume fraction index, load combination and initial geometric imperfections on thermo-electro-mechanical post-buckling behavior. Thermo-electro-elastic analysis of thick-walled functionally graded piezoelectric cylindrical shell was studied by rahimi et al. [11]. Power law function was used for description of functionality for all mechanical, thermal and electrical properties of material. Linear and nonlinear thermo-elastic analysis of functionally graded piezoelectric spherical shell was investigated based on electro-elastic and Maxwell relations by Arefi and Khoshgoftar [12] and also by Arefi and Nahas [13].

Arefi et al. [16] studied the effect of axially variable thermal and mechanical loads on the 2D thermoelastic response of FG cylindrical shell. Hamida et al. [17] provided a sensitivity analysis for identification of key input parameters affecting energy conversion factor of flexoelectric materials. The numerical results indicated that the flexoelectric constants are the most dominant factors influencing the uncertainties in the energy conversion factor. Ghasemi et al. [18] presented a computational methodology for topology optimization of multi-material-based flexoelectric composites. They provided some numerical examples for two-, three- and four-phase flexoelectric composites to demonstrate the flexibility of the model that can be obtained using multi-material topology optimization for flexoelectric composites. Other related works to optimization and computational methods of flexoelectric and piezoelectric structures were studied by various researchers [19-20].

Literature review on the thermo-elastic analysis of temperature dependent materials and structures was presented in Introduction. Although some important works on the temperature dependent materials and structures have been performed by various researchers, based on author's knowledge, there is no published works on the electro-thermo-elastic analysis of thick-walled spherical shell made of functionally graded temperature dependent materials subjected to thermal, electrical and mechanical loads. Innovative aspects of this research are the study of the dependence of all material properties on temperature, and considering the temperature gradient. It can be seen that considering temperature dependency would lead to significant changes

of all material properties and consequently important changes in electro-thermo-elastic results.

In this article, linear temperature dependency is used for all mechanical, thermal and electrical temperature-dependent material properties. In addition, power law function is used for functionally graded piezoelectric materials. The division method is applied for solution of the two second-order governing equations with variable coefficients. The numerical results are presented to show the influence of temperature dependency and functionality of piezoelectric material on the radial displacement, radial and circumferential stress, electric field and temperature distribution.

2. Fromulation

The governing equations of thermo-electro-elastic analysis of functionally graded piezoelectric spherical shell are presented in this section. The spherical shell is subjected to thermal and mechanical loads at inner and outer radii (see Fig. 1).

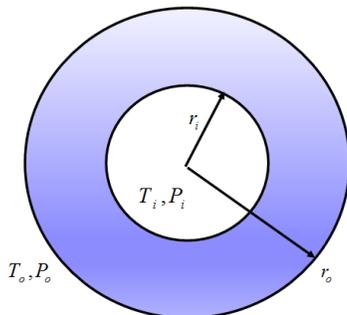The heat conduction equation in spherical coordinate system is defined as [12]:

$$\frac{1}{r^2}\frac{\partial}{\partial r}\left(K_T r^2 \frac{\partial T}{\partial r}\right) = 0 \quad r_i \leq r \leq r_o \tag{1}$$

The spherical shell is assumed to be made of functionally graded temperature dependent materials. Based on this assumption, the thermal conductivity coefficient is considered as [14, 15]:

$$K_T(r,T) = (p_1 T(r) + p_0)r^k \tag{2}$$

In Eq. (2), p_0, p_1 are two constants showing the temperature dependency. Solution of heat conduction equation may be obtained by substitution of thermal conductivity coefficient and two times integration as follows:

$$T(r) = \frac{-p_0 + \sqrt{2r^{-k-1}a_1 p_1 + 2a_2 p_1 + p_0{}^2}}{p_1} \tag{3}$$

Fig. 1. The schematic of a functionally graded piezoelectric spherical shell made of temperature-dependent materials

The temperature distribution can be obtained by applying the necessary boundary conditions. Applying the boundary conditions $T(r_i) = T_i \quad T(r_o) = T_o$ to temperature distribution found in Eq. (3) would yield the integration constants as follows:

$$\begin{cases} a_1 = -\frac{1}{2}\frac{f_1}{r_o{}^{-k-1} - r_i{}^{-k-1}} \\ a_2 = \frac{1}{2}\frac{f_2}{r_o{}^{-k-1} - r_i{}^{-k-1}} \end{cases} \tag{4}$$

where:

$$f_1 = p_1 T_i{}^2 - p_1 T_o{}^2 + 2p_0 T_i - 2p_0 T_o$$

$$f_2 = p_1 T_i{}^2 r_o{}^{-k-1} - r_i{}^{-k-1} T_o{}^2 p_1 + 2p_0 T_i r_o{}^{-k-1} - 2r_i{}^{-k-1} T_o p_0$$

In this stage and after completion of thermal analysis, the electro-thermo-elastic relations could be presented. The stress-strain and electric displacement relations by considering the thermal and electrical effects are developed in spherical coordinate system as follows [12]:

$$\sigma_{rr} = c_{rr}\varepsilon_{rr} + 2c_{r\theta}\varepsilon_{\theta\theta} - e_{rr}E_r - \beta_r T$$
$$\sigma_{\theta\theta} = c_{r\theta}\varepsilon_{rr} + (c_{\theta\theta} + c_{\phi\phi})\varepsilon_{\theta\theta} - e_{r\theta}E_r - \beta_\theta T \tag{5}$$
$$D_r = \eta E_r - pT + e_{rr}\varepsilon_{rr} + 2e_{r\theta}\varepsilon_{\theta\theta}$$

in which, $\sigma_{ij}, \varepsilon_{ij}, E_i, T, D_r$ are stress, strain, electric field, temperature distribution and electrical displacement. In addition, c_{ij}, e_{ij} are stiffness and piezoelectric coefficients. Furthermore, η is the dielectric constant and p is the pyroelectric constant. β_i, p could be obtained from [12]:

$$\beta_r = c_{rr}\alpha_r + c_{r\theta}\alpha_\theta$$
$$\beta_\theta = c_{r\theta}\alpha_r + c_{\theta\theta}\alpha_\theta \tag{6}$$
$$p = e_{rr}\alpha_r + e_{r\theta}\alpha_\theta$$

Due to symmetric distribution of all mechanical and electrical components, the circumferential component of the electrical displacement D_θ, is zero. For a symmetric spherical structure, only nonzero displacement component is radial displacement. Therefore, the strain-displacement and electric field-electric potential relations are defined as [12]:

$$\varepsilon_{rr} = \frac{\partial u}{\partial r}, \varepsilon_{\theta\theta} = \varepsilon_{\phi\phi} = \frac{u}{r}$$
$$E_r = -\frac{\partial \varphi}{\partial r} \tag{7}$$

In which, φ is the electric potential distribution. Substitution of strain and electric field components into stress and electric displacement relations leads to updated form of these relations as follows:

$$\sigma_{rr} = c_{rr}\frac{\partial u}{\partial r} + 2c_{r\theta}\frac{u}{r} + e_{rr}\frac{\partial \varphi}{\partial r} - (c_{rr}\alpha_r + c_{r\theta}\alpha_\theta)T$$

$$\sigma_{\theta\theta} = c_{r\theta}\frac{\partial u}{\partial r} + (c_{\theta\theta} + c_{\Phi\Phi})\frac{u}{r} + e_{r\theta}\frac{\partial \varphi}{\partial r} - (c_{r\theta}\alpha_r + c_{\theta\theta}\alpha_\theta)T$$

$$D_r = -\eta\frac{\partial \varphi}{\partial r} - (e_{rr}\alpha_r + e_{r\theta}\alpha_\theta)T + e_{rr}\frac{\partial u}{\partial r} + 2e_{r\theta}\frac{u}{r}$$

(8)

The equilibrium and Maxwell relations are utilized to derive the governing equations. These relations are presented as:

$$\frac{\partial \sigma_{rr}}{\partial r} + 2\frac{\sigma_{rr} - \sigma_{\theta\theta}}{r} = 0$$

$$\frac{\partial D_r}{\partial r} + \frac{2D_r}{r} = 0$$

(9)

Before derivation of governing equations, the functionally graded temperature dependent material properties should be expressed. These relations are expressed as [1,3,4]:

$$e_{rr} = (-3 \times 10^{-4}T(r) - 0.1082)r^k$$

$$e_{r\theta} = (-10^{-5}(T(r))^2 + 6.3 \times 10^{-3}T(r) - 0.8701)r^k$$

$$\alpha_r = -3 \times 10^{-7}T(r) + 2 \times 10^{-4}$$

$$\alpha_\theta = -3 \times 10^{-7}T(r) + 2 \times 10^{-4}$$

$$c_{rr} = (-4 \times 10^7 T(r) + 2 \times 10^{10})r^k$$

(10)

$$c_{r\theta} = (-10^7 T(r) + 7 \times 10^9)r^k$$

$$c_{\theta\theta} = (-10^7 T(r) + 5 \times 10^9)r^k$$

$$c_{\Phi\Phi} = (-10^7 T(r) + 4 \times 10^9)r^k$$

$$\eta = (6 \times 10^{-12}T(r) - 9 \times 10^{-10})r^k$$

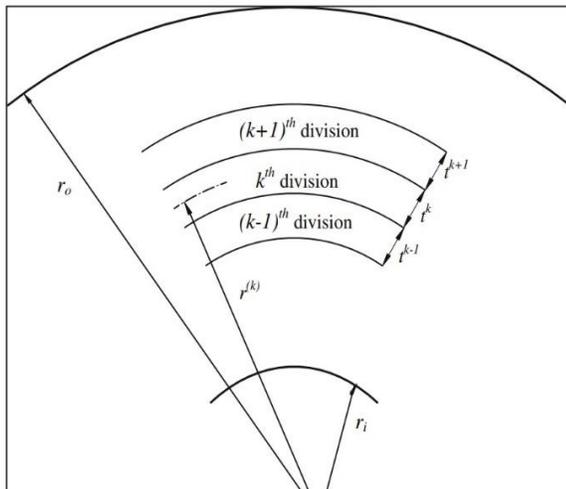The stress components and electric displacement relations are derived as Eq. (11):

Fig. 2. The schematic of a sub-divided functionally graded piezo-electric cylinder

$$\sigma_{rr} = r^k \begin{bmatrix} \left(-4\times10^7 T + 2\times10^{10}\right)\dfrac{\partial u}{\partial r} \\ -\left(2\times10^7 T - 14\times10^9\right)\dfrac{u}{r} \\ -\left(3\times10^{-4} T + 0.1082\right)\dfrac{\partial \varphi}{\partial r} \\ -\left(15T^3 - 18100T^2 + 5.4\times10^6 T\right) \end{bmatrix}$$

$$\sigma_{\theta\theta} = r^k \begin{bmatrix} \left(-10^7 T + 7\times10^9\right)\dfrac{\partial u}{\partial r} \\ -\left(2\times10^7 T - 9\times10^9\right)\dfrac{u}{r} \\ -\left(10^{-5} T^2 - 6.3\times10^{-3} T + 0.8701\right)\dfrac{\partial \varphi}{\partial r} \\ -\left(6T^3 - 7600T^2 + 2.4\times10^6 T\right) \end{bmatrix}$$

(11)

$$D_r = -r^k \begin{bmatrix} \left(6\times10^{-10} T - 9\times10^{-8}\right)\dfrac{\partial \varphi}{\partial r} \\ -\left(1.9\times10^{-4} - 3\times10^{-12} T^4 + 3.8\times10^{-9} T^3\right) \\ +1.5\times10^{-6} T^2 + \left(3\times10^{-4} T + 0.1\right)\dfrac{\partial u}{\partial r} \\ +2\left(10^{-5} T^2 - 6.3\times10^{-3} T + 0.87\right)\dfrac{u}{r} \end{bmatrix}$$

Substitution of stress and electric displacement relations into equilibrium and Maxwell relations would result in final governing equations. Presentation of governing equations is not provided due to very large terms.

3. Solution procedure

The solution procedure is developed in this section based on division method. This method is applied for solution of differential equations with variable coefficients.

In this method, the variable coefficient differential equations are evaluated at the middle of each layer by substitution of $\bar{r}_i = \frac{r_i + r_{i+1}}{2}$ into governing equations (see Fig. 2). After evaluation of governing equations for each layer, the obtained governing equations are solved. The compatibility relations between two adjacent layers should be written as:

$$u_{n-1}(r = r_{n-1}) = u_n(r = r_{n-1})$$

$$u'_{n-1}(r = r_{n-1}) = u'_n(r = r_{n-1})$$

$$\varphi_{n-1}(r = r_{n-1}) = \varphi_n(r = r_{n-1})$$

$$\varphi'_{n-1}(r = r_{n-1}) = \varphi'_n(r = r_{n-1})$$

(12)

For instance, the governing equations for the first layer are derived as:

$$\begin{cases} -0.22\dfrac{\partial^2 \varphi}{\partial r^2} + 0.21\dfrac{\partial \varphi}{\partial r} - 1.7 \times 10^9 + 4.26 \times 10^{10}\dfrac{\partial u}{\partial r} \\[2mm] +4.05 \times 10^9 \dfrac{\partial^2 u}{\partial r^2} + 1.32 \times 10^{10} u = 0 \\[2mm] -1.47 \times 10^{-7}\dfrac{\partial^2 \varphi}{\partial r^2} + 6.4 \times 10^{-7}\dfrac{\partial \varphi}{\partial r} - 0.06 + 0.42\dfrac{\partial u}{\partial r} \\[2mm] -0.22\dfrac{\partial^2 u}{\partial r^2} + 3.4 u = 0 \end{cases} \quad (13)$$

Solving the governing equations of layer 1 leads to following one:

$$\varphi_1 = -3.12 c_1 e^{-0.32r} - 0.098 c_2 e^{-10.2r}$$
$$+0.23 c_3 e^{4.34r} - 6.1 \times 10^5 r + c_4$$

$$u_1 = 2.7 \times 10^{-12} c_3 e^{4.34r} - 2.1 \qquad (14)$$
$$\times 10^{-7} c_1 e^{-0.32r}$$
$$+8.7 \times 10^{-8} c_2 e^{-10.2r} + 0.13$$

Evaluation of solution for each layer (as presented above) and applying the continuity equations (as presented by Eq. 12) gives a system of algebraic relation in terms of c_i. In addition, the boundary conditions for P(VDF-TrFE) copolymers at inner and outer layers are expressed as:

$$r_i = 1, \ r_o = 1.1$$
$$\sigma_{rr}(r = r_i) = -5 \times 10^6, \ \ \varphi(r = r_i) = 0$$
$$\sigma_{rr}(r = r_o) = 0, \varphi(r = r_o) = 0 \qquad (15)$$
$$T(r = r_i) = T_i = 403.15$$
$$T(r = r_o) = T_o = 303.15$$

4. Numerical results and discussion

Before presentation of full numerical results, the effect of temperature dependency is studied on the results rather than the cases that temperature independency is assumed. Fig. 3 shows the temperature distribution along the radial direction based on two cases: first for temperature dependent materials and second, for temperature independent materials.

The comparison between temperature distribution for the temperature-dependent and temperature-independent materials indicates that the temperature calculated for temperature-dependent materials is slightly less than the one for temperature-independent materials.

Radial distribution of radial stress is presented in Fig. 4 for two aforementioned cases. It is observed that the applied boundary conditions are satisfied at inner and outer surfaces. In addition, one can conclude that the radial stress for temperature-independent case is greater than the one for temperature-dependent case. Fig. 5 shows the radial distribution of circumferential stress for tempera-

ture-dependent/independent material cases. It is observed that considering the temperature-independency, the slope of circumferential stress is reducted and tends to uniform condition along the thickness direction. Fig. 6 shows the radial variation of electric field for temperature-dependent and independent material cases. The similar behavior of Fig. 5 could be observed in the results of Fig. 6.

Fig. 7 shows the radial distribution of electric potential for temperature-dependent and independent material cases. It is observed that the absolute value of the electrical potential for the temperature-dependent properties is lower than that of the independent temperature. Shown in Fig. 8 is the radial distribution of radial displacement in terms of various in-homogeneous index k. it is observed that with increase of in-homogeneous index k, the radial displacement is decreased significantly. One can conclude that with increase of in-homogeneous index k, the stiffness of structure is increased which leads to significant decrease in radial displacements.
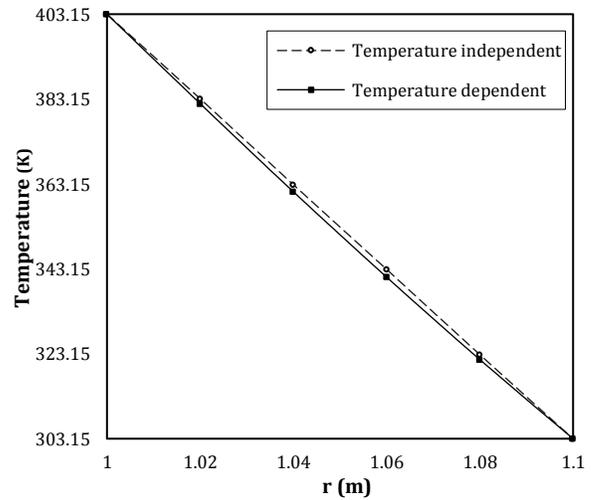

Fig. 3. The radial distribution of temperature distribution based on temperature dependent and independent materials
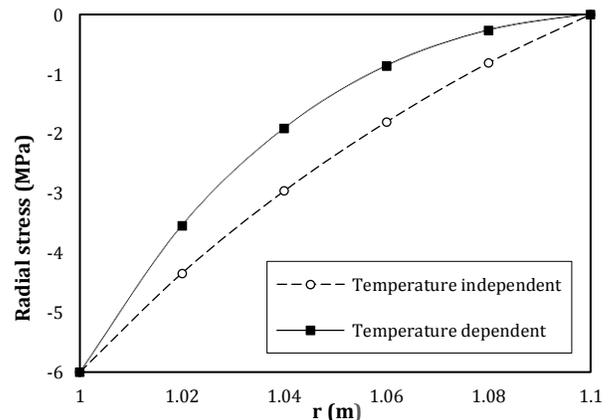

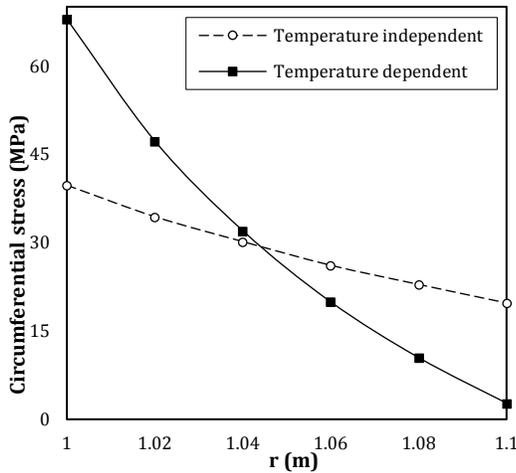**Fig. 4.** The radial distribution of radial stress based on temperature dependent and independent materials

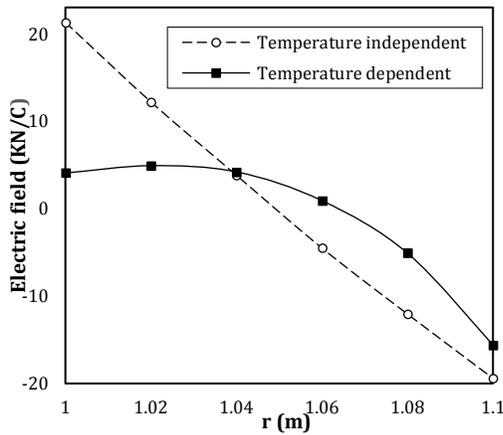**Fig.5.** The radial distribution of circumferential stress based on temperature-dependent and independent materials

Fig. 6. The radial distribution of electric field based on temperature-dependent and independent materials
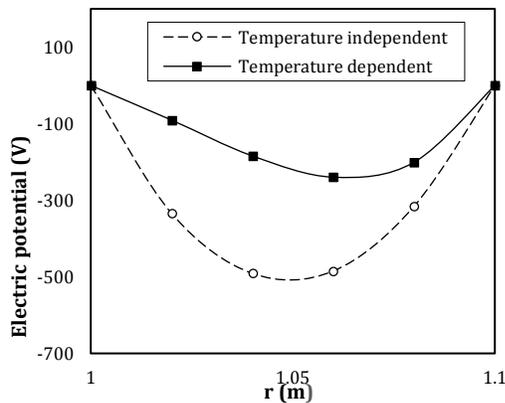

Fig. 7. The radial distribution of electric potential based on temperature-dependent and independent materials

Fig. 9 shows the variation of electric potential along the thickness direction for various values of in-homogeneous index k. The numerical results indicate the sign of electric potential changes from negative to positive for higher values of in-homogeneous index k. Fig. 10 shows the radial distribution of the electric field along the thickness direction for various values of in-homogeneous in-

dex k. Fig. 11 shows the radial distribution of the temperature along the thickness direction for various values of in-homogeneous index k. It could be observed that with increase of in-homogeneous index k, the temperature decreased.

5. Conclusions

The effect of temperature-dependency was studied on the thermo-electro-elastic results of a functionally graded spherical shell subjected to thermal, mechanical and electrical loads. It was assumed that all mechanical and thermal material properties are graded along the thickness direction based on power law function and also temperature dependent. The governing equations were derived based on equilibrium and Maxwell relations considering thermal and electrical effects. The division method was employed for solving the governing equations with variable coefficients. The numerical results were presented to show the influence of temperature-dependency of all mechanical, thermal and electrical loads and in-homogeneous index. The main results of this work are classified as follows:
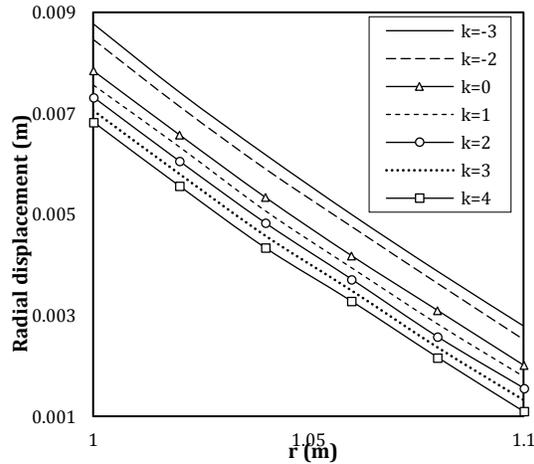

Fig. 8. The radial distribution of radial displacement for various in-homogeneous indices
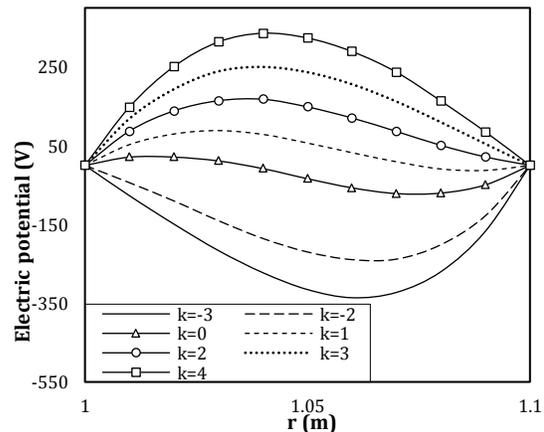

Fig. 9. The radial distribution of electric potential for various values of in-homogeneous index k
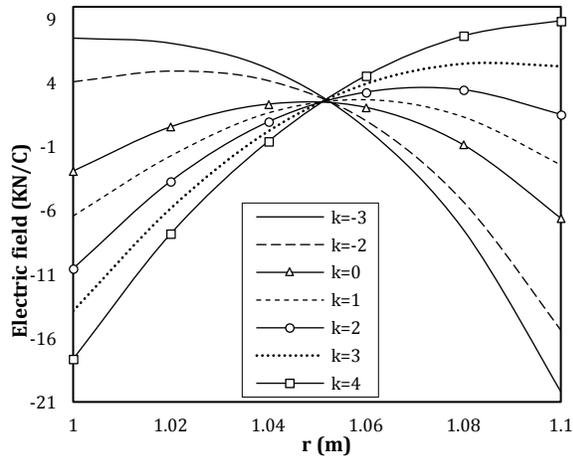
Fig. 10. The radial distribution of electric field for various values of in-homogeneous index k
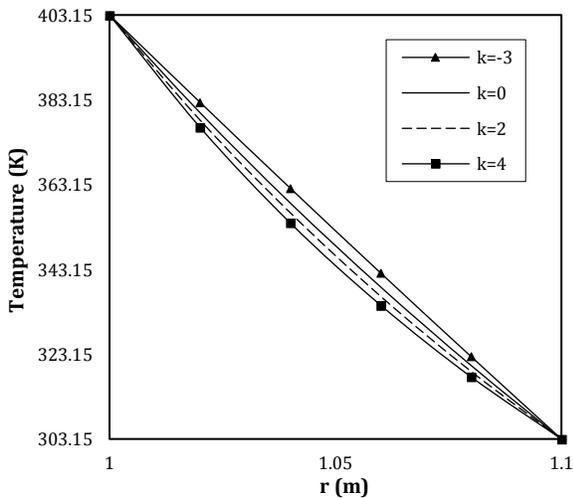

Fig. 11. The radial distribution of temperature for various values of in-homogeneous index k

The numerical results indicated that considering the temperature-dependency would lead to significant changes of thermo-electro-elastic results. One can conclude that the radial displacement and stress, temperature distribution and electric field for temperature-independent case is significantly greater than that of temperature dependent material. It is concluded that for temperature-independent case, the effect of thermal strains leads to significant increase of deformations and stresses in spherical shell.

Variation of in-homogeneous index leads to significant changes and different behaviors of outputs such as radial displacement, radial and circumferential stresses, temperature distribution and electric field. The numerical results indicate that with increase of in-homogeneous index, the radial displacement and stress, electric potential and temperature would significantly decrease. Furthermore, the behavior of circumferential stress and electric field depend on the radial location study in which at lay-

ers near the inner surface, these components decrease with increase of in-homogeneous index while at layers near the outer surface would increase. Temperature, the radial stress and radial displacement for temperature-independent case is greater than one for temperature-dependent case.

References

[1] Teyssedre G, Lacabanne C. Study of the thermal and dielectric behavior of P (VDF-TrFE) copolymers in relation with their electroactive properties. *Ferroelectrics* 1995; 171(1): 125-144.

[2] Tanigawa Y, Akai T, Kawamura R, Oka N. Transient heat conduction and thermal stress problems of nonhomogeneous plate with temperature-dependent material problems. *J Therm Stresses* 1996; 19(1): 77-102.

[3] Omote K, Ohigashi H, Koga K. Temperature dependence of elastic, dielectric, and piezoelectric properties of "single crystalline"films of vinylidene fluoride trifluoroethylene copolymer. *J Appl Phys* 1997; 81(6): 2760-2769.

[4] Wong Y, Hui N, Ong E, Chan H, Choy C. Specific heat and thermal diffusivity of vinylidene fluoride/trifluoroethylene copolymers. *J Applied Poly Sci* 2003; 89(12): 3160-3166.

[5] Shen HS. Thermal postbuckling behavior of functionally graded cylindrical shells with temperature-dependent properties. *Int J Solids Struc* 2004; 41(7): 1961-1974.

[6] Liew KM, Yang J, Kitipornchai S. Thermal Post-Buckling of Laminated Plates Comprising Functionally Graded Materials with Temperature-Dependent Properties. *J Appl Mech* 2005; 71(6): 839-850.

[7] Kim YW. Temperature dependent vibration analysis of functionally graded rectangular plates. *J Sound Vib* 2005; 284(3–5): 531-549.

[8] Yang J, Liew KM, Wu YF, Kitipornchai S. Thermo-mechanical post-buckling of FGM cylindrical panels with temperature-dependent properties. *Int J Solids Struct* 2006; 43(2): 307-324.

[9] Shen HS. Thermal postbuckling behavior of shear deformable FGM plates with temperature-dependent properties. *Int J Mech Sci* 2007; 49(4): 466-478.

[10] Shariyat M. Dynamic buckling of suddenly loaded imperfect hybrid FGM cylindrical shells with temperature-dependent material properties under thermo-electro-mechanical loads. *Int J Mech Sci* 2008; 50(12): 1561-1571.

[11] Rahimi GH, Arefi M, Khoshgoftar MJ. Electro elastic analysis of a pressurized thick-walled functionally graded piezoelectric cylinder using the first order shear deformation theory and energy method. *Mechanika* 2012; 18(3): 292-300.

[12] Arefi M, Khoshgoftar MJ. Comprehensive piezo-thermo-elastic analysis of a thick hollow spherical shell. *Smart Struct Sys* 2014; 14(2): 225-246.

[13] Arefi M, Nahas I. Nonlinear electro thermo elastic analysis of a thick spherical functionally graded piezoelectric shell. *Compos Struct* 2014; 118: 510-518.

[14] Arefi M, Rahimi GH, Khoshgoftar MJ. Optimized design of a cylinder under mechanical, magnetic and thermal loads as a sensor or actuator using a functionally graded piezomagnetic material. *Int J Phys Sci* 2011; 6(27): 6315-6322.

[15] Arefi M, Rahimi GH. Thermo elastic analysis of a functionally graded cylinder under internal pressure using first order shear deformation theory. *Sci Res Essays* 2011; 5(12): 1442-1454.

[16] Arefi M, Faegh RK, Loghman A. The effect of axially variable thermal and mechanical loads on the 2D thermoelastic response of FG cylindrical shell. *J Therm Stresses* 2016; 39(12): 1539-1559.

[17] Hamdia KM, Ghasemi H, Zhuang X, Alajlan N, Rabczuk T. Sensitivity and uncertainty analysis for flexoelectric nanostructures. *Comput Meth Appl Mech Eng* 2018; 337: 95-109.

[18] Ghasemi H, Park HS, Rabczuk T. A multi-material level set-based topology optimization of flexoelectric composites. *Comput Meth Appl Mech Eng* 2018; 332: 47-62.

[19] Ghasemi H, Park HS, Rabczuk T. A level-set based IGA formulation for topology optimization of flexoelectric materials. *Comput Meth Appl Mech Eng* 2017; 313: 239-258.

[20] Thai TQ, Rabczuk T, Zhuang X. A large deformation isogeometric approach for flexoelectricity and soft materials. *Comput Meth Appl Mech Eng* 2017; 341: 718-739.